Bioinorganic clays: synthesis and characterization of amino- and polyamino acid intercalated layered double hydroxides

Nicola T. Whilton, Paula J. Vickers and Stephen Mann*

School of Chemistry, University of Bath, Bath, UK BA2 7AY

Negatively charged amino acids (aspartic acid, glutamic acid) and a related polymer, poly(α,β-aspartate), have been intercalated within the gallery spaces of layered double hydroxides. Synthesis of these bioinorganic nanocomposites was achieved *via* co-precipitation involving simultaneous formation of the inorganic layers and intercalation of the anionic species. *In situ* thermal polymerization of pre-intercalated aspartate monomers affords a second route to the poly(α,β-aspartate)-containing hybrid material.

The layered double hydroxides (LDHs) consist of inorganic brucite-like $M^{II}(OH)_2$ layers that are positively charged due to partial substitution of the framework divalent cations with trivalent metal ions. Overall electrical neutrality is maintained by the presence of anions (and water)[1] within the gallery spaces between the inorganic sheets. The general composition of these intercalation materials can be represented as $[M^{II}_{1-x}M^{III}_x(OH)_2]^{x+}\cdot[(A^{m-})_{x/m}\cdot nH_2O]$ where M^{II} is a divalent cation such as Mg, Ni, Cu or Zn, M^{III} is a trivalent metal ion such as Al, Cr, Fe, V, or Ga, and $A_{x/m}$ an anion of charge m such as CO_3^{2-}, Cl^-, SO_4^{2-} or NO_3^-. The naturally occurring mineral, hydrotalcite, has a representative formula unit of $[Mg_6Al_2(OH)_{16}][CO_3]\cdot 4H_2O$, although the value of x can vary between 0.16 and 0.45 in synthetic derivatives.[2] These inorganic layered materials are often termed 'anionic clays', complementing the more conventional cationic clays and related lamellar compounds (*e.g.* smectite clays, phosphates and phosphonates of tetravalent metals). Interest in clays and inorganic lamellar compounds lies in their potential technological applications as catalysts, ion-exchangers, optical hosts and, more recently, as important components in the fabrication of new ceramic-based materials and nanocomposites.[3]

The anion-exchange properties of LDHs[4] can be exploited for the post-synthesis incorporation of small, negatively charged organic molecules into the gallery spaces between the brucite layers. A direct synthesis approach has recently been successful for the preparation of well ordered LDH materials containing intercalated anions such as terephthalate,[5] long-chain fatty acids,[6] organic dyes[7] and phthalocyanine-type molecules.[8,9] However, the fabrication of LDH nanocomposites with polymeric guest molecules has afforded limited success, primarily because the methods generally employed for polymer incorporation in other layered inorganic host materials[10] have not been applicable. Most notably, the exfoliation/adsorption approach,[11–13] widely utilized for the fabrication of polymer–clay hybrids of the smectite- and MS_2-type, is not a viable synthetic route for polymer–LDH nanocomposites as the high charge density on the LDH layers prevents exfoliation of the sheets. To date, poly(aniline)–LDH[14] and poly(acrilonitrile)–LDH[15] nanocomposites have been prepared by *in situ* polymerization of pre-intercalated monomers. A direct synthesis approach, similar to that used for the incorporation of small organic molecules, has been used to intercalate poly(vinyl alcohol) into a Ca–Al–LDH with the formation of a well ordered layered nanocomposite.[16,17] More recently, nanostructural materials based on $Mg_4Al_2(OH)_{12}\cdot nH_2O$ and related LDH sheet structures, and the ionomers poly(acrylic acid), poly(vinyl sulfonate) and poly(styrene sulfonate), have been directly synthesized by coprecipitation from solutions containing the desired polymer as co-solute.[18]

This study is concerned with the synthesis and characterization of layered double hydroxides (LDHs) intercalated with anionic amino acids such as aspartate or glutamate, or a polyamino acid derivative, poly(α,β-aspartate). We show that these new bioinorganic hybrid materials can be produced by direct synthesis. We also describe the formation of a layered nanocomposite containing poly(α,β-aspartate) macromolecules using an approach based on the *in situ* polymerization of intercalated aspartate monomers.

Experimental

Materials

Organic and inorganic reagents were of analytical grade (Aldrich) and used without further purification. Sodium hydroxide pellets were obtained from BDH. A solution of sodium poly(α,β-aspartate) (27% m/m in H_2O; M_r *ca.* 1000; *ca.* 62 aspartate residues per molecule) was obtained as a gift from BP International. Doubly distilled water was further purified by passing through a Stillplus Purite water system.

Preparation of carbonate-containing layered double hydroxide (LDH)

A layered magnesium/aluminium double hydroxide containing intercalated carbonate (Mg–Al–CO_3–LDH) was prepared using a standard aqueous precipitation and thermal crystallization method.[19] Typically, a solution containing $Mg(NO_3)_2\cdot 6H_2O$ (0.58 g, 2.3 mmol) and $Al(NO_3)_3\cdot 9H_2O$ (0.43 g, 1.1 mmol) in 18 ml doubly distilled water was added dropwise over 1 h to a vigorously stirred freshly prepared solution containing NaOH (0.32 g, 8.0 mmol, pH = 12) and Na_2CO_3 (0.24 g, 2.3 mmol) in 10 ml doubly distilled water. During addition there was no change in pH. The resultant gel was aged with stirring at 65 °C for 24 h. A white solid was subsequently isolated by filtration under suction and dried in a vacuum oven at 70 °C for 24 h. Elemental analysis gave 2.5%C, 4.0%H, 0.2%N, 62.0%O, 20.0%Mg and 11.3%Al.

Preparation of aspartate- and glutamate-containing LDHs

Aspartate– and glutamate–LDHs were prepared by reacting a mixed-metal nitrate solution with a basic solution containing the organic dianion.[5] The free organic acid (D,L-aspartic acid, D-glutamic acid; 1.1 mmol) was dissolved in a freshly prepared solution of NaOH (10 mmol in 10 ml doubly distilled water) and the resulting solution stirred under nitrogen. A solution containing $Mg(NO_3)_2\cdot 6H_2O$ (0.58 g, 2.3 mmol) and $Al(NO_3)_3\cdot 9H_2O$ (0.43 g, 1.1 mmol) in 18 ml doubly distilled

water was deaerated with nitrogen before slow addition to the organic anion-containing solution. The pH of the reaction mixture remained fairly constant at 11.5–12 during the addition. The resulting precipitate was aged at 65 °C for 24 h and then filtered in air under suction and dried at 70 °C under vacuum for a further 24 h. Elemental analysis gave 6.8%C, 4.3%H, 3.5%N, 57.7%O, 17.3%Mg and 10.4%Al for the aspartate-containing LDH, and 7.1%C, 4.7%H, 2.9%N, 59.4%O, 17.0%Mg and 9.3%Al for glutamate–LDH.

Preparation of polyaspartate-containing LDH

The preparation of polyaspartate-intercalated LDHs was achieved by two synthetic procedures: (*a*) by *in situ* thermal polycondensation of an aspartate-containing LDH, and (*b*) *via* direct intercalation of the preformed polymer present as co-solute in the basic reaction solution.

(*a*) Thermal polycondensation of aspartate-containing LDH. Typically, a sample (0.5–1.0 g) of the dried aspartate–LDH was heated in a furnace at 220 °C for 24 h in air. Upon removal from the furnace the crucible and sample were allowed to cool slowly in a dessicator in air to room temperature. The product was yellow–pale brown. The organic content of the heated materials was calculated as 21–25 mass%. The heat-treated sample was dispersed in 20 ml doubly distilled water under an argon purge and the pH of the solution adjusted to 11.0 by the addition of 10 mol dm^{-3} NaOH solution. The reaction mixture was stirred at 60 °C for 1 h, during which the pH was maintained at 11.0 by further addition of NaOH solution. Upon cooling to room temperature the solution was neutralized by the addition of HCl and the solid product isolated by centrifugation and washed with doubly distilled water. Elemental analysis of the heated sample gave 7.7%C, 3.8%H, 3.9%N, 57.1%O, 16.9%Mg and 9.9%Al, and after base hydrolysis, 7.3%C, 4.2%H, 1.2%N, 60.5%O, 16.8%Mg and 10.0%Al.

(*b*) Direct intercalation. Polyaspartate solution (0.75 g of a 27% m/m polymer solution: 1.5 mmol aspartate monomers, [Asp*]) was stirred in a freshly prepared solution of NaOH (7.5 mmol in 10 ml water) under nitrogen. The pH of the resulting solution was *ca.* 12. A solution containing $Mg(NO_3)_2{\cdot}6H_2O$ (0.29 g, 1.2 mmol) and $Al(NO_3)_3{\cdot}9H_2O$ (0.22 g, 0.6 mmol), previously purged with nitrogen, was added dropwise to the vigorously stirred polymer solution. The resulting suspension was aged at 65 °C for 24 h and the tan coloured product was dried under vacuum at 50 °C for 24 h. Elemental analysis gave 15.3%C, 4.4%H, 4.4%N, 57.0%O, 10.4%Mg and 8.6%Al.

Characterization

X-Ray powder diffraction (XRD) data were collected on a Phillips PW1130 diffractometer using Cu-Kα radiation (λ = 1.5405 A). FTIR spectra were recorded on samples pressed into KBr discs using a Nicolet 51OP FTIR spectrophotometer. Electron microscopy was performed on ground samples, dispersed by sonication in ethanol or water, using a JEOL 1200EX microscope with attached scanning imaging device. Thermal analyses of powdered samples up to temperatures of 600 °C were carried out at a ramp rate of 5 °C min^{-1} in flowing N_2 using a Perkin-Elmer Delta Series 7 instrument. Organic contents were calculated from the C : N ratio obtained from microanalyses of the samples performed on a Varian AA-275 Series spectrophotometer. Atomic absorption spectroscopy was used to determine the Mg and Al contents.

Results and Discussion

Aspartate- and glutamate-containing LDHs

The XRD pattern for the carbonate–LDH showed characteristic reflections which corresponded to an interlayer spacing of 7.6 A [Table 1, Fig. 1(a)]. By contrast, the aspartate– and glutamate–LDHs [Fig. 1(b) and (c)] showed expanded structures with broad (003) diffraction peaks at 11.1 and 11.9 A, respectively (Table 1). These expanded interlayer separations are consistent with the intercalation of the organic anions within the gallery spaces of the LDH. Weak (006) and (00,12) reflections were also observed, indicating that the amino acid intercalated LDHs were single phases with significant stacking disorder. Assuming a thickness of 4.8 A for the brucite layer, the gallery spacings were approximately 6.3 and 7.1 A for aspartate– and glutamate–LDHs, respectively, compared with a carbonate–LDH gallery height of 2.8 A. These values suggest a monolayer arrangement for the intercalated amino acids, with the carboxylates of individual molecules bridging adjacent layers of the inorganic framework.

Calculated chemical compositions for the as-synthesized intercalated LDHs are shown in Table 2. The organic content of the aspartate- and glutamate-containing materials was typically 20% by mass. Nitrate ions were also co-intercalated within the gallery spaces. This was confirmed by FTIR spectroscopy (see below) and was consistent with a broad XRD peak at 4.2 A [Fig. 1(b), (c)] which was attributed to disordered layers of intercalated nitrate anions (d_{006} for pure NO_3–LDH = 4.0 A) within the amino acid–LDH materials. The compositional data demonstrate that the amount of organic and inorganic anions incorporated into the LDH materials is stoichiometrically related to the net positive charge generated by Al substitution in the inorganic layers. In addition, the data indicate that the acidic amino acids were incorporated as dianionic species, consistent with the highly alkaline [pH = 12; $pK_a(NH_3^+) = 10.0$] reaction conditions.

For all synthetic procedures, an initial mole ratio of Mg/Al = 2 was charged to the reaction vessel. The resulting Mg/Al ratios in the precipitated products differed according to the nature of the intercalated anions. For the purely inorganic carbonate–LDH, a ratio of Mg/Al of 2.8 indicated an incomplete precipitation of aluminium ions. In comparison, the corresponding ratios in the aspartate and glutamate samples were slightly lower than the theoretical value (Table 2), indicating an enrichment of the trivalent cation in the brucite layers. This suggests that the composition of the brucite layers initially formed can be influenced by host–guest interactions that are presumably taking place prior to assembly of the double hydroxide layers. For example, differences in the stability

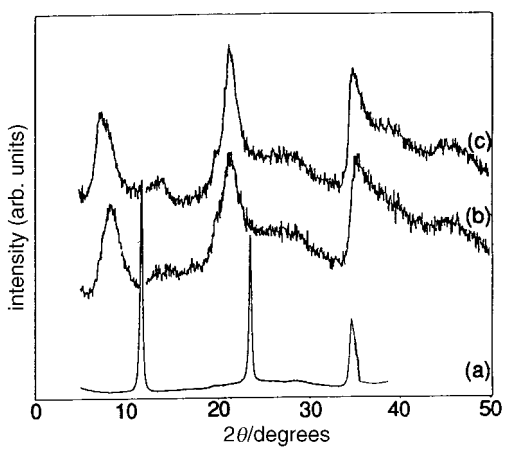

Fig. 1 Powder XRD patterns for (a) carbonate–LDH, (b) aspartate–LDH and (c) glutamate–LDH

Table 1 XRD data (d/Å) for synthesized LDHs (ht = heated)

	d_{003}	d_{006}	d_{009}	d_{006}[a]	$d_{00,12}$	d_{012}	gallery height[b]
CO_3–LDH	7.6	3.8	—	—	—	2.6	2.8
Glu–LDH	11.9	6.0	—	4.2	3.1	2.6	7.1
Asp–LDH	11.1	5.7	—	4.2	2.9	2.5	6.3
ht–Asp–LDH	9.0	—	—	4.3	—	2.5	4.2
ht–Asp–LDH + OH	12.2	6.3	—	3.9	—	2.6	7.4
ht–CO_3–LDH	6.8	3.4	—	—	—	2.6	2.0
polyAsp–LDH	15.1	7.7	5.8	—	3.9	—	10.3

[a]Values assigned to intercalated nitrate/carbonate. [b]Assumes a thickness for the brucite layer of 4.8 Å.

Table 2 Compositional data for synthesized LDH materials[a]

	chemical composition	Mg/Al ratio
CO_3–LDH	$Mg_{1.15}Al_{0.4}(OH)_{3.08}[CO_3]_{0.2}[NO_3]_{0.01}\cdot 0.5H_2O$	2.8
Asp–LDH	$Mg_{0.71}Al_{0.38}(OH)_{2.18}[Asp]_{0.14}[NO_3]_{0.10}\cdot 0.6H_2O$	1.9
Glu–LDH	$Mg_{0.7}Al_{0.34}(OH)_{2.05}[Glu]_{0.12}[NO_3]_{0.10}\cdot 0.9H_2O$	1.8
polyAsp–LDH	$Mg_{0.43}Al_{0.32}(OH)_{2.05}[Asp^*]_{0.32}\cdot 1.1H_2O$	1.2

[a][Asp] = aspartate dianion, [Glu] = glutamate dianion, [Asp*] = polyaspartate monomer.

constants of Al^{3+} and Mg^{2+} complexes of the amino acid dianions might favour the partial fractionation of the more highly charged cationic species. However, it is known that LDH materials with low crystallinity often have low Mg/Al ratios,[20] suggesting that the trivalent enrichment could be a general kinetic effect.

FTIR spectra of the aspartate– and glutamate–LDHs showed absorption bands corresponding to the intercalated organic dianions (Fig. 2). Characteristic alkyl C—H stretches were observed in the region 3000–2800 cm^{-1} of both spectra and the RCO_2^- asymmetric and symmetric stretches at 1590 and 1400 cm^{-1}, respectively, were also evident. Co-intercalated nitrate anions gave a very intense absorption at 1385 cm^{-1}. A broad absorption between 3600 and 3200 cm^{-1} was associated with the stretching mode of hydrogen-bonded hydroxy groups from both the hydroxide layers and interlayer water. Peaks at 650 and 460 cm^{-1} were assigned to the metal–oxygen modes of the LDH sheets.

Thermogravimetric analysis traces for the carbonate–LDH showed a distinctive reduction in mass between 80 and 200 °C (15 mass%) owing to loss of surface adsorbed and interlayer water. A major mass loss was observed at 280 °C, continuing up to 500 °C, owing to concomitant dehydroxylation of the inorganic layers and decomposition of intercalated carbonate anions (*ca.* 30 mass%)[21] [Fig. 3(a)]. In contrast, the aspartate–LDH underwent a more gradual mass loss from room temperature up to *ca.* 330 °C (25 mass%) [Fig. 3(b)] owing to both dehydration of the hydroxide layers and polycondensation of the intercalated aspartate monomers (see below). At 330 °C, the onset of a rapid and major mass loss ensued, continuing up to 500 °C as dehydroxylation and partial decomposition of organics occurred (30 mass% loss). The corresponding DSC trace (data not shown) showed two endotherms centred at 360 and 430 °C owing to dehydroxylation and organic decomposition, respectively.

Electron microscopy revealed significant differences in the morphologies of the carbonate- and amino acid-intercalated LDHs. The bead-like structure of the carbonate–LDH [Fig. 4(a), 5(a)] was evident in both scanning and transmission electron micrographs, which showed discrete, regular sized particles of *ca.* 0.1 μm dimensions. In contrast, the aspartate–LDH afforded non-uniform irregular aggregates (< 1.0 μm in size) of plate-like morphology [Fig. 4(b), 5(b)]. Layering within the sample was evident and coherent lattice fringes were occasionally imaged [Fig. 5(c)]. These results

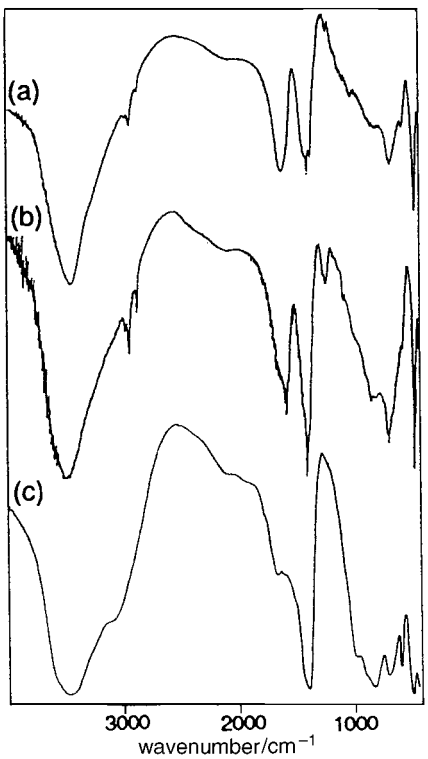

Fig. 2 FTIR spectra for (a) aspartate–LDH, (b) glutamate–LDH and (c) carbonate–LDH

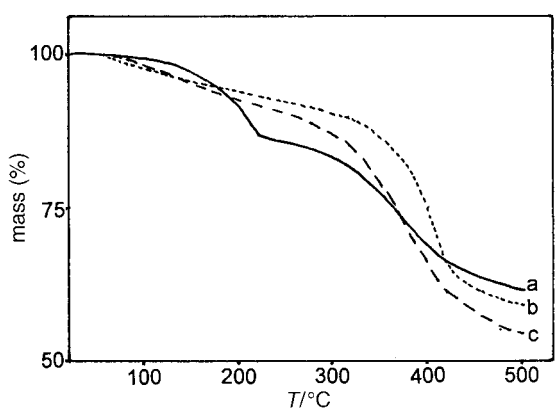

Fig. 3 TG profiles for (a) carbonate–LDH, (b) aspartate–LDH and (c) polyaspartate–LDH (prepared by direct synthesis)

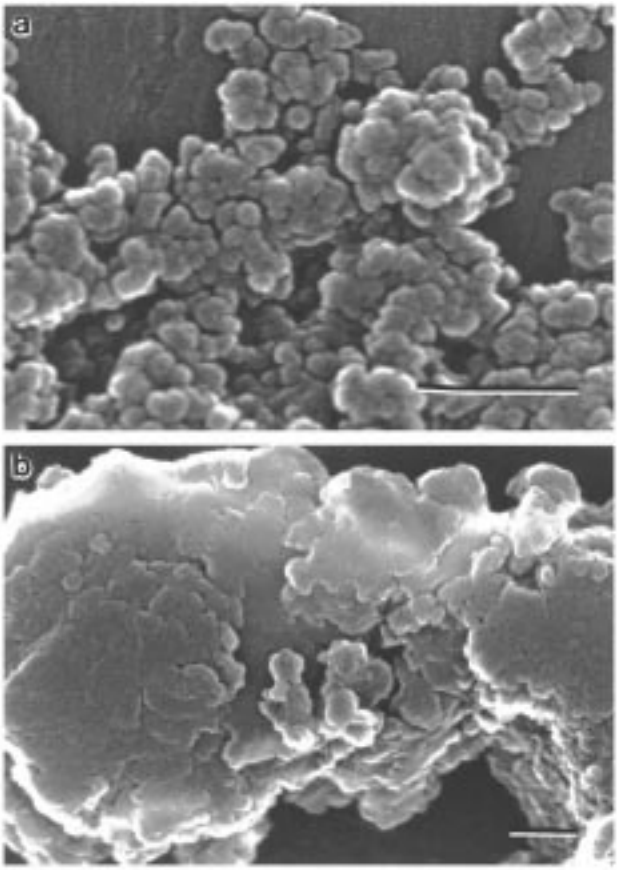

Fig. 4 SEM images for (a) carbonate–LDH and (b) aspartate–LDH. Scale bars = 500 nm.

indicate that the texture and morphology of LDH materials can be influenced by the nature of the intercalated anion. The insertion of new growth units into a developing crystal surface, as well as the aggregation behaviour of primary particles, can be influenced by properties such as spatial charge distribution, lattice periodicity and the stereochemical disposition of surface groups. Guest anions can therefore make a significant contribution to the interfacial interactions associated with crystallization. For example, the basal (001) face of the LDH structure appears to be preferentially stabilized in the presence of aspartate, with the result that plate-like primary particles are formed.

Polyaspartate-containing LDH

(*a*) Synthesis by *in-situ* polymerization. Thermal treatment of the white aspartate–LDH ($d_{003} = 11.1$ A) at 200 °C for 48 h resulted in a single-phase yellow material with a decreased d_{003} spacing of 9.0 A, corresponding to a reduction in the interlayer separation of 2.1 A [Table 1, Fig. 6(a)]. The d_{003} peak width was comparable with that of the aspartate–LDH material before heating, but no d_{006} reflection was observed. By comparison, a heated sample of carbonate–LDH showed only a small contraction in d_{003} from 7.6 to 6.8 A and the d_{006} reflection was still present. The decreases in basal spacing and structural order can be attributed to the loss of intercalated water molecules and, in the case of aspartate–LDH, also to the polycondensation of the organic monomers within the gallery spaces of the LDH. The organic content of the heated samples remained between 20 and 25 mass% (Table 2) indicating no significant de-intercalation of the organic molecules.

Electron microscopy of aspartate–LDH following thermal treatment and before treatment with NaOH showed little change in morphology of the clay particles. Surface cracking could be observed in the SEM (data not shown), presumably

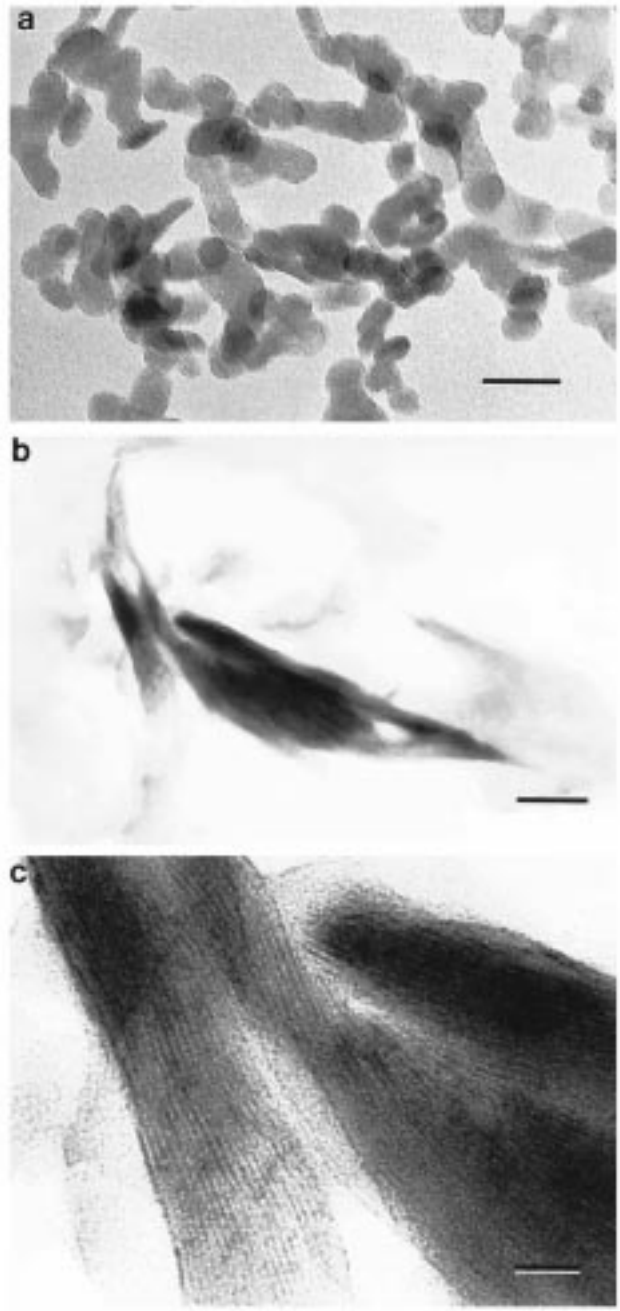

Fig. 5 TEM images for (a) carbonate–LDH and (b) aspartate–LDH. Scale bars = 50 nm. (c) High magnification view of an area of (b) showing lattice fringes ($d = 10.8$ A). Scale bar = 10 nm.

owing to loss of water during dehydration, but the overall plate-like shape and aggregated texture remained.

Subsequent treatment of the heat-treated sample with sodium hydroxide yielded a material which exhibited a broad d_{003} reflection [Table 1, Fig. 6(b)] with a peak maximum at 12.2 A, and the reappearance of the d_{006} reflection, suggesting further rearrangement/conversion of the intercalated organic species. In addition, the 4.2 A reflection attributed to intercalated nitrate was no longer observed, and a new peak at 3.9 A was assigned to the presence of disordered brucite layers containing carbonate anions. Thus, treatment with NaOH results in facile exchange of intercalated nitrate for carbonate, presumably by rehydration in the presence of high concentrations of dissolved CO_2. This interpretation is consistent with the NMR and FTIR data described below. Moreover, the increase in the interlayer spacing to a value larger than the unheated aspartate–LDH suggests that condensation reac-

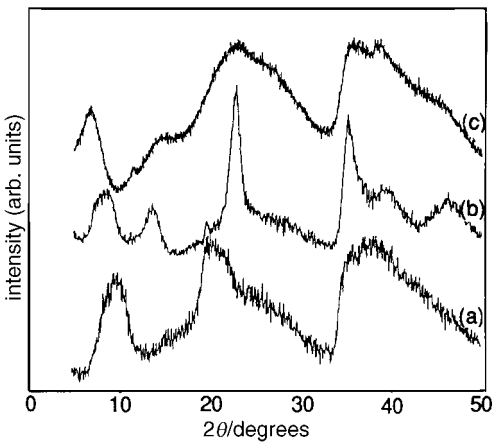

Fig. 6 Powder XRD patterns for (a) aspartate–LDH after heat treatment at 220 °C for 24 h, (b) aspartate–LDH after heating and treatment with NaOH and (c) polyaspartate–LDH prepared by direct synthesis

tions may have occurred within the gallery spaces. The thermal polymerization of aspartic acid at 200 °C followed by treatment with base is a well documented method of forming poly(α,β-aspartate). The reaction proceeds *via* a polysuccinimide intermediate which rearranges to give polyaspartate (Scheme 1).[22,23]

The decrease in the interlayer spacing after dry thermal treatment, and subsequent expansion following reaction with aqueous NaOH supports the implication that initial heating of the organo–LDH brings about *in situ* polymerization of the aspartate monomers to produce intercalated polyimides, which subsequently undergo ring-opening by hydrolysis.

Supporting evidence for polycondensation of the intercalated monomers was provided by solid-state ^{13}C NMR spectroscopy. The spectrum of the as-synthesized aspartate–LDH afforded signals consistent with the presence of aspartate dianions [δ 180 (CO_2^-), 54 (CHN), 41 (CH_2)], and carbonate (δ 170) [Fig. 7(a)]. Following heat treatment, a new resonance at δ 175 was observed in the form of a shoulder to the δ 180 peak [Fig. 7(b)]; this peak was characteristic of an amide linkage [C(=O)−N] and was also observed in the solution ^{13}C NMR spectrum of pristine polyaspartate [δ 180 (COO^-), 174 [C(=O)−N], 54 (CHN) and 40 (CH_2)]. However, an additional resonance at δ 166 suggested the presence also of an imide [(C=O)−NR−(C=O)], although this peak is not reported in the NMR spectrum for polysuccimide.[24] Subsequent treatment with NaOH gave a spectrum consistent with further reaction of the imide intermediate; in particular, the δ 174 resonance (amide linkage) was now well resolved against the δ 179 carboxylate peak, and the δ 166 (imide) resonance was absent [Fig. 7(c)]. The spectrum also contained several new resonances between δ 15 and 60, suggesting that a number of species were formed in the hydrolysis reaction. A sharp resonance at δ 170 due to inorganic carbonate, which was small in the heated aspartate-containing LDH prior to base hydrolysis, was also observed.

There was little change in the FTIR spectrum of the sample

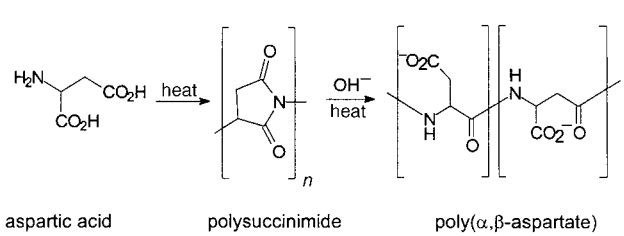

Scheme 1 Thermal polycondensation of aspartic acid to poly(α,β-aspartate)

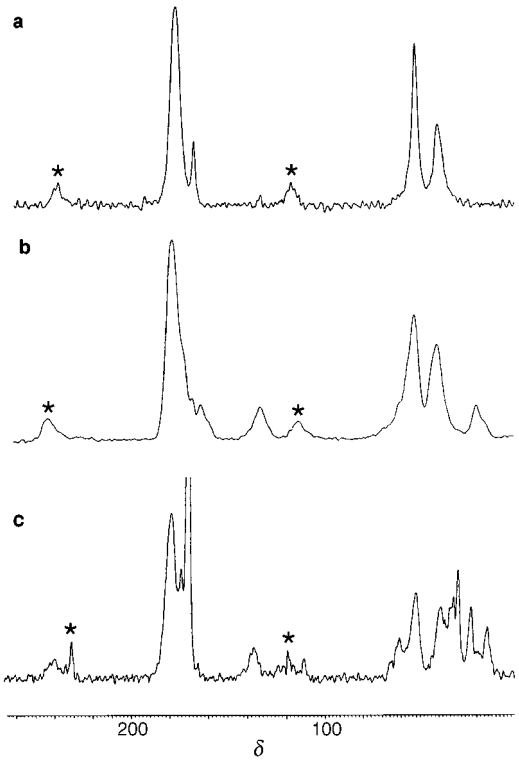

Fig. 7 ^{13}C CP MAS NMR spectra for (a) aspartate–LDH, (b) aspartate–LDH after heat treatment, and (c) aspartate–LDH after heating and treatment with NaOH. Asterisks indicate spinning side-bands.

after heating [Fig. 8(a)], when compared to the as-synthesized aspartate–LDH [Fig. 2(a)]. Absorptions due to alkyl C−H groups were still evident between 2800 and 2900 cm^{-1}, but the unambiguous assignment of polymer residues was not possible. Other assignments could be made for intercalated nitrate ions (1385 cm^{-1}), and the metal–oxygen stretching modes (460 and 650 cm^{-1}). Following base hydrolysis, an intense but broad absorption peak at 1500–1700 cm^{-1} was attributed to carbonyl resonances from amide (1650 cm^{-1}) and carboxylate groups (*ca.* 1580 cm^{-1}) of polyaspartate, whilst a broad peak of comparable intensity (1380–1450 cm^{-1}) was consistent with the symmetric stretching mode of carboxylate groups (1410 cm^{-1}), and inorganic carbonate (1390 cm^{-1}) [Fig. 8(b)]. Metal–oxygen stretching absorptions were also observed.

***(b)* Synthesis by direct intercalation.** Direct intercalation of polyaspartate by co-precipitation afforded an organo–LDH with an average interlayer separation of 15.1 A [Table 1, Fig. 6(c)]. The XRD pattern also showed broad peaks for the d_{006} and d_{009} spacings, and a very broad reflection centred at 3.9 A which could be $d_{00,12}$ or d_{006} of highly disordered carbonate-intercalated layers, or both. However, elemental analysis of the polymer–LDH gave a typical chemical composition, $Mg_{0.43}Al_{0.31}(OH)_{1.48}[Asp^*]_{0.31}\cdot 0.8H_2O$ (Table 2). Assuming 62 Asp* monomers per polymer molecule, this gives a molar stoichiometry of $[polyaspartate]_{0.006}$, with an organic content between 20 and 35% by mass. The data indicate that the singly charged aspartate side residues of polyaspartate are the charge balancing species, and no evidence for the incorporation of other inorganic anions was observed. The Mg/Al ratio was 1.2, indicating that Al^{3+} incorporation into the inorganic layers was more favourable than in the case of the dianionic aspartate– and glutamate–LDHs, which again suggests a

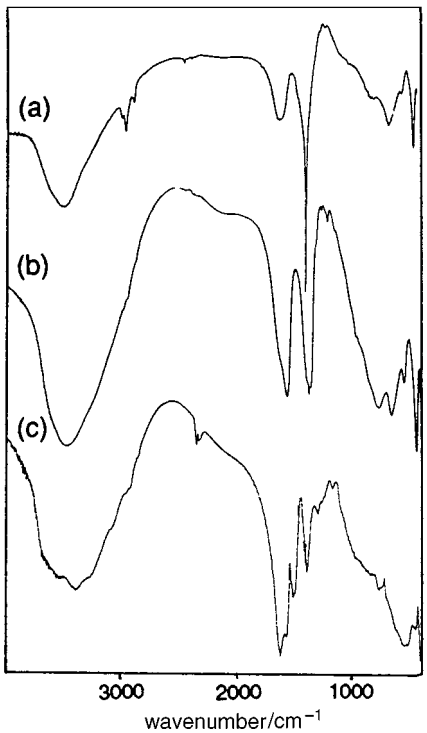

Fig. 8 FTIR spectra for (a) aspartate–LDH after heat treatment, (b) aspartate–LDH following thermal and base treatment, and (c) polyaspartate–LDH prepared by direct synthesis

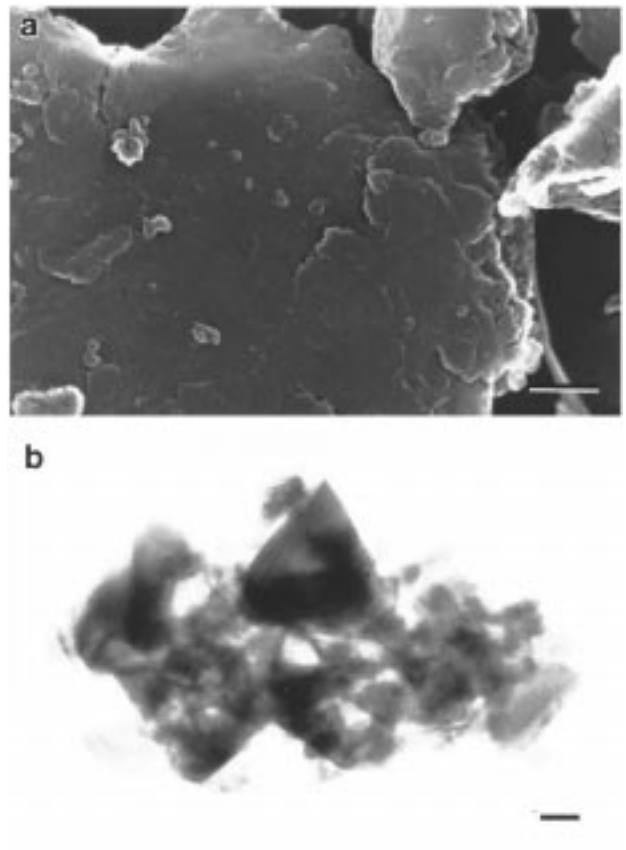

Fig. 9 (a) SEM image (scale bar = 1 μm) and (b) TEM image (scale bar = 50 nm) for polyaspartate–LDH prepared by direct synthesis

degree of guest-assisted cationic selectivity in the synthesized clay.

FTIR spectroscopy showed characteristic frequencies associated with the intercalated polyaspartate macromolecules [Fig. 8(c)]. Major assignments included those for N—H (3500 cm^{-1}), C=O (1650 cm^{-1}), CO_2^- (1580, 1410 cm^{-1}), and N—H (1520 cm^{-1}). The clearly resolved absorption peaks arising from the intercalated organic species reflect in part the higher organic content of the preformed polymer intercalation material. The spectrum correlated well with absorptions assigned to intercalated polyaspartate in the spectrum of the heat-treated, base-hydrolysed aspartate–LDH sample [Fig. 8(b)]. The results therefore support the hypothesis that in the latter case, *in situ* reaction with NaOH is required to convert thermally derived intercalated polyimide intermediates to the ring-opened polyaspartate product.

TG profiles showed an almost linear loss in mass of 13% from room temperature up to 280 °C [Fig. 3(c)], which was attributed to dehydration of the layered double hydroxide. At 280 °C, a more rapid and sustained decrease in mass began, corresponding to dehydroxylation and loss of intercalated organics (30–50 mass%), levelling out around 600 °C. It was impossible to distinguish between the onset of these two events. However, the onset of decomposition of a pristine sodium polyaspartate sample was found by TG and DSC to be at *ca.* 420 °C.

The polyaspartate–LDH formed by direct intercalation consisted of irregularly shaped aggregates of plate-like particles, often exceeding 1.0 μm in size, and with very smooth surface textures [Fig. 9(a)]. TEM images showed crystals often with well defined edges [Fig. 9(b)].

Conclusions

In this paper we have shown that organo-intercalated LDH materials, containing acidic amino or polyamino acids, can be prepared by direct synthesis. Aspartate and glutamate monomers can be intercalated at 20 mass% to produce LDHs with expanded interlayer spacings and modified texture. Poly(α,β-aspartate) can also be intercalated by coprecipitation to give a laminated nanocomposite with *ca.* 15 A repeat spacing. Thermal polycondensation of intercalated aspartate monomers, followed by base hydrolysis, results in a LDH material containing poly(α,β-aspartate) and unreacted polyimide intermediates. These new bioinorganic hybrid materials might have uses as organo-clays with bioactive, biocompatible or biodegradable properties.

We thank B. Chapman (University of Bath) for XRD, BP International for the gift of poly(α,β-aspartate), Dr. D. C. Apperley (University of Durham) for NMR spectroscopy, and English China Clays International for TG–DSC analysis. We thank the NERC for support of a postgraduate studentship to N.T.W.

References

1 W. T. Reichle, *CHEMTECH*, 1986, **16**, 58.
2 K. Allmann, *Chimia*, 1970, **24**, 99.
3 F. Cavani, F. Trifiro and A. Vaccari, *Catal. Today*, 1991, **11**, 173.
4 M. Meyn, K. Beneke and G. Lagaly, *Inorg. Chem.*, 1990, **29**, 5201.
5 M. A. Drezdon, *Inorg. Chem.*, 1988, **27**, 4628.
6 L. Raki, D. G. Rancourt and C. Detellier, *Chem. Mater.*, 1995, **7**, 221.
7 I. Y. Park, K. Kurado and C. Kato, *J. Chem. Soc., Dalton Trans.*, 1990, 3071.
8 K. A. Carrado, J. E. Forman, R. E. Botto and R. E. Winans, *Chem. Mater.*, 1993, **5**, 472.
9 S. Bonnet, C. Forano, D. de Roy, J. P. Besse, P. Maillard and M. Momenteau, *Chem. Mater.*, 1996, **8**, 1962.
10 R. Krishnamoorti, R. A. Vaia and E. P. Giannelis, *Chem. Mater.*, 1996, **8**, 1728.
11 J. P. Lemmon and M. M. Lerner, *Chem. Mater.*, 1994, **6**, 207.
12 J. Wu and M. M. Lerner, *Chem. Mater.*, 1993, **5**, 835.
13 R. Bissessur, M. G. Kanatzidis, J. L. Schindler and C. R. Kannewurf, *J. Chem. Soc., Chem. Commun.*, 1993, 1582.

14 T. Challier and R. C. T. Slade, *J. Mater. Chem.*, 1994, **4**, 367.
15 Y. Sugahara, N. Yokoyama, K. Kurado and C. Kato, *Ceram. Int.*, 1988, **14**, 163.
16 P. B. Messersmith and S. I. Stupp, *J. Mater. Res.*, 1992, **7**, 2599.
17 P. B. Messersmith and S. I. Stupp, *Chem. Mater.*, 1995, **7**, 454.
18 C. O. Oriakhi, I. V. Farr and M. M. Lerner, *J. Mater. Chem.*, 1996, **6**, 103.
19 W. T. Reichle, *J. Catal.*, 1985, **94**, 547.
20 L. Albiston, K. R. Franklin, E. Lee and J. B. A. F. Smeulders, *J. Mater. Chem.*, 1996, **6**, 871.
21 V. R. L. Constantino and T. J. Pinnavaia, *Inorg. Chem.*, 1995, **34**, 883.
22 E. Katchalski, *Adv. Protein Chem.*, 1951, **6**, 123.
23 J. E. Donachy and C. S. Sikes, *J. Polym. Sci., Part A: Polym. Chem.*, 1994, **32**, 789.
24 S. K. Wolk, G. Swift, Y. H. Paik, K. M. Yocom, R. L. Smith and E. S. Simon, *Macromolecules*, 1994, **27**, 7613.

Paper 7/01237C; *Received* 21*st February*, 1997